Russian Chemical Reviews **83** (3) 183 – 195 (2014) © 2014 Russian Academy of Sciences and Turpion Ltd

DOI 10.1070/RC2014v083n03ABEH004427

Heterogeneous photocatalysts in organic synthesis

M Cherevatskaya, B König

Faculty of Chemistry and Pharmacy, University of Regensburg
Universitätstrasse 31, 93049 Regensburg, Germany

The review deals with the application of inorganic semiconductors in organic synthesis. Although the majority of reported reactions still aim at the photocatalytic decomposition of organic compounds, the number of examples in synthetic applications is growing. The principal mechanisms of heterogeneous semiconductor photocatalysis are considered and examples illustrating the use of inorganic semiconductors in organic synthesis are given. The discussion is arranged according to the required excitation wavelength (UV or visible light) and to the new bond that is formed (carbon – carbon or carbon – heteroatom bond).
The bibliography includes 47 references.

Contents

I. Introduction 183
II. Typical reaction mechanisms of heterogeneous photocatalysis 183
III. UV light-mediated heterogeneous photocatalysis 185
IV. Visible light-mediated heterogeneous photocatalysis 189
V. Conclusion 194

I. Introduction

The idea of using photochemical processes to synthesize useful organic chemicals was already mentioned long ago in Giacomo Ciamician's report in *Science* in 1912 where he raised the question '*Would it not be advantageous to make better use of radiant energy?*' He predicted the rapid development of methods that use abundant and renewable solar energy instead of harmful reagents in organic synthesis. Since then, photochemistry has developed into a mature field of chemistry. The majority of the experiments use direct excitation of molecules by UV light. Sensitization or photocatalytic methods, in contrast, apply dye molecules, which are excited by visible light irradiation and transfer energy or an electron from the excited state to the molecule to be converted. Such photocatalysts or sensitizers can be either soluble in the reaction media or insoluble leading to homogeneous or heterogeneous reaction mixtures. Widely used homogeneous visible light absorbing photocatalysts are organic dyes such as Eosin Y, Rose Bengal, Nile Red or Rhodamine B and ruthenium(II), iridium(III) or copper(I) metal complexes. Typical heterogeneous photocatalysts are organic and inorganic semiconductors. We discuss in this review synthetically useful C – C and C – heteroatom bond formation methods mediated by heterogeneous inorganic photocatalysts. The earliest applications of heterogeneous photocatalysis aim for the degradation of organic pollutants or dyes in wastewater streams, water or air or for the photocatalytic splitting of water into hydrogen and oxygen. Only recently, heterogeneous photocatalysis was more widely applied to the organic synthesis of fine chemicals.[2, 3]

Our survey covers the application of UV- and visible light-absorbing semiconductors. Typical UV-absorbing semiconductors are TiO_2, ZnS and ZnO. Their wide band gap makes them both strong oxidizing and strong reducing agents. Examples of visible light-absorbing semiconductors are CdS, surface modified TiO_2 or $PbBiO_2Br$. The redox potential of all heterogeneous semiconductors is pH-dependent in water and again different in organic solvents.

M Cherevatskaya Dr. rer. nat., Faculty of Chemistry and Pharmacy, University of Regensburg. Tel. (49-941) 943 45 75,
e-mail: maria.cherevatskaya@gmail.com
B König Dr. rer. nat., Full Professor, Faculty of Chemistry and Pharmacy, University of Regensburg. Tel. (49-941) 943 45 75,
e-mail: burkhard.koenig@ur.de
Current research interests: heterogeneous photocatalysts absorbing visible radiation.

Received 16 September 2013
Uspekhi Khimii **83** (3) 183 – 195 (2014)

II. Typical reaction mechanisms of heterogeneous photocatalysis

The mechanism of reactions photocatalyzed by inorganic semiconductors (SC) comprises several key steps given in Eqns (1) – (3) and illustrated in Fig. 1. Light absorption induces the electron/hole separation [Eqn (1)]. The corresponding energy levels are located at the surface and not in the bulk, as may be assumed from the simplified Fig. 1. The electron/ hole separation could be followed by back electron transfer to the valence band, thus regenerating the semiconductor ground state [Eqn (2)], or the electron – hole pair

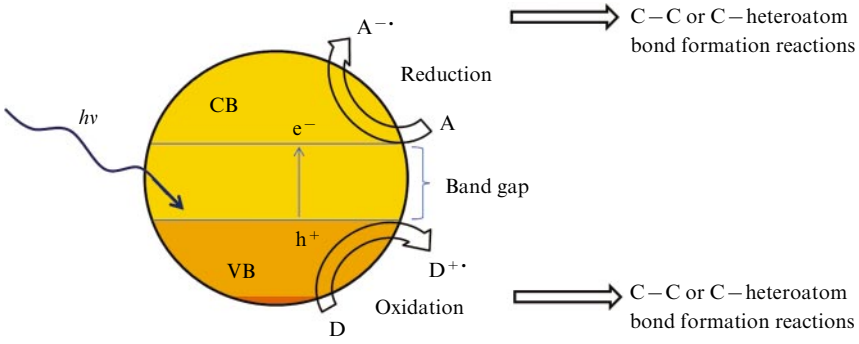


Figure 1. Redox reactions of a light-excited semiconductor with electron donor (D) and electron acceptor (A) molecules.

may undergo subsequent redox reactions with suitable electron donor and acceptor molecules [Eqn (3)].

$$SC \xrightarrow{h\nu} SC^*(e^-,h^+) \quad (1)$$

$$SC^*(e^-,h^+) \longrightarrow SC + h\nu/\text{heat} \quad (2)$$

$$SC^*(e^-,h^+) + A + D \longrightarrow SC + A^{-\bullet} + D^{+\bullet} \quad (3)$$

Hence, a successful organic synthesis using inorganic semiconductor photocatalysts depends on several parameters:

1. The band gap of the semiconductor determines its absorption wavelength. Only a photon with the appropriate energy can excite an electron from the valence band (VB) to the conduction band (CB). The wavelength λ must have larger or equal energy as compared to the band gap energy (E_{BG}):

$$h\nu = \frac{hc}{\lambda} \geqslant E_{BG}$$

where h is the Planck constant, ν the frequency of the photon and c is the speed of light. The photon energy together with the potential of the valence band allows an estimation which chemical processes as half reactions may be feasible (see Fig. 1). The generated hole at the valence band (VB) corresponds to the available oxidation potential energy. The reduction potential of the excited electron, in turn, is determined by the potential of the CB and can be calculated from the following equation:

$$E_{CB}[B] = E_{VB}[B] + \frac{E_{BG}[eV]}{e^0[\text{the number of e}]}$$

where E_{CB} is the conduction band lower edge energy, E_{VB} is is the valence band upper edge energy, e^0 corresponds to the number of excited electrons.[4]

2. The redox potentials of the reaction partners are crucial. An appropriate electron acceptor ($A/A^{-\bullet}$) should have a reduction potential lower than the CB lower edge of the semiconductor photocatalyst. On the other hand, the electron donor ($D/D^{+\bullet}$) oxidized by the excited photocatalyst should be higher in energy than the photocatalyst VB upper edge. Using the Rehm–Weller equation one can calculate the Gibbs free energy indicating whether the reaction is thermodynamically allowed.

3. When planning a synthesis based on heterogeneous semiconductor photocatalysis, the challenge is to translate the transient charge separation into an irreversible and selective reaction. After the semiconductor excitation, we can expect different ways how the system loses the obtained energy [see Eqns (2) and (3)]. The easiest way for the excited electron in the CB is to recombine back to the VB [see Eqn (2)] and after this recombination, the electron and the hole are lost for a redox reaction. However, the desired way is the interfacial electron/hole transfer at the solid–liquid or solid–gas interface and consecutive redox reactions. In general, the electron/hole recombination time is dependent on the nature of the material and is in the range of nano- or microseconds. In the case of TiO_2, the recombination process is very fast and takes place in $\sim$30 ps.

To classify the bond formation reactions arising from primary redox species ($A^{-\bullet}$ and $D^{+\bullet}$), the group of Kisch suggested the terms 'type A photocatalysis' and 'type B photocatalysis.' The type A photocatalysis affords two different products, one reduced and one oxidized [Eqn (4)], while type B photocatalysis leads to one single addition product *via* an intermolecular bond formation [Eqn (5)].[5]

$$A + D \xrightarrow[h\nu]{SC} B_{red} + C_{ox} \text{ (type A photocatalysis)} \quad (4)$$

$$A + D \xrightarrow[h\nu]{SC} A-D \text{ (type B photocatalysis)} \quad (5)$$

It is commonly assumed that species A and D are adsorbed at the semiconductor (SC) surface to allow for electron transfer at high rates, but there are cases where the substrates cannot contact the semiconductor surface. These are examples of aerobic oxidation reactions where the electron transfer to and from adsorbed oxygen and water generates short-lived reactive intermediates that diffuse to the substrates.

Figure 2 summarizes the reported valence band and band gap energies for typical semiconductors in several solvents. These potentials are correlated with the redox potentials of key steps of homogeneous photocatalytic reactions involving ruthenium or iridium complexes or organic dyes such as eosin Y. The broad red and blue lines indicate the approximate potentials required for the corresponding reduction or oxidation steps in synthesis. This can be used to select the appropriate heterogeneous semicon-

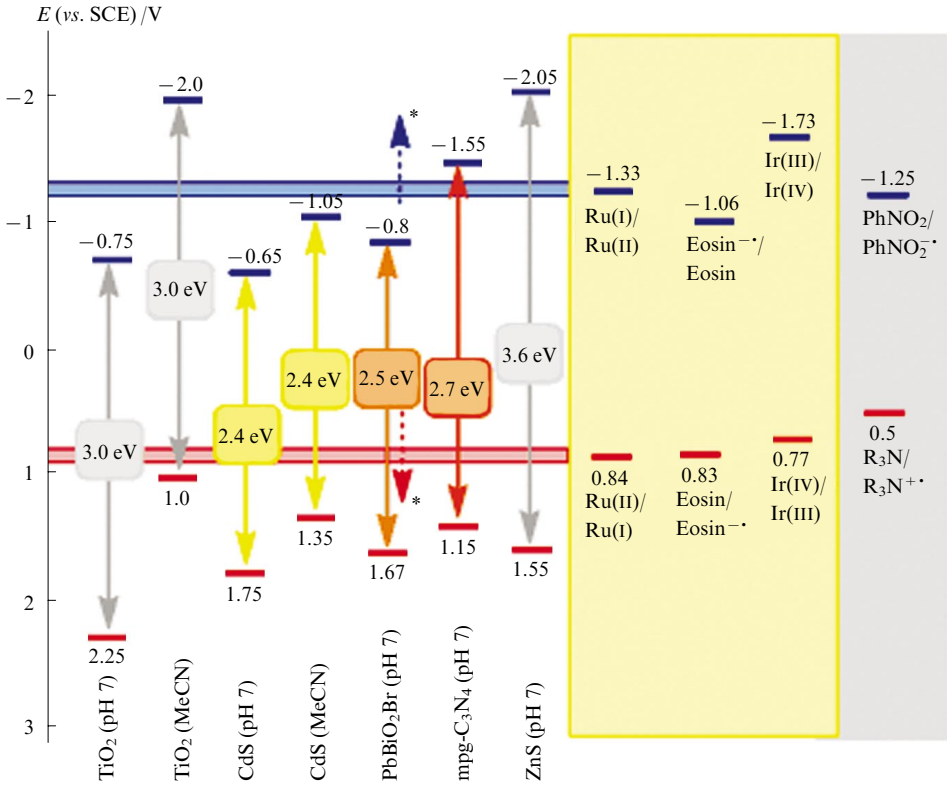


Figure 2. Redox potentials and E_{BG} values for common semiconductors compared with redox potentials of some sensitizers.[6] The asterisks mark the estimated values for $PbBiO_2Br$ in MeCN. The values for Ru refer to $[Ru(bipy)_3]^{2+}$, those for Ir correspond to *fac*-$[Ir(ppy)_3]$ (bipy is 2,2′-bipyridine, ppy is phenylpyridyl). SCE is the saturated calomel electrode; mpg-C_3N_4 is mesoporous graphilized C_3N_4.

ductor to replace a precious homogeneous photoredox catalysts such as ruthenium-tris-bipyridine.

A key feature of photocatalyzed bond formation reactions is that they often proceed under mild conditions and are suitable for conversion of non-activated precursors. Photocatalysis, therefore, serves as a worthy alternative to thermal processes.

III. UV light-mediated heterogeneous photocatalysis

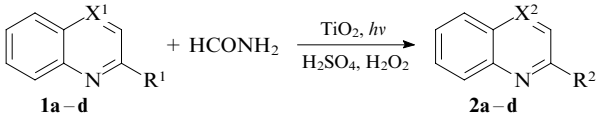
1. Carbon–carbon bond forming reactions

The functionalization of C–H bonds is an ambitious task. Electrochemically[7,8] and thermally generated radicals[9–11] have been used but photocatalytically generated radicals seem to be a promising alternative due to the rapidly growing achievements in this field. Successful examples of such transformations employed a UV light-absorbing homogeneous photocatalyst, tetrabutylammonium decatungstate (TBADT), in the alkylation of α,β-unsaturated ketones or alkenes and other examples.[12–16]

The heterogeneous photocatalyst TiO_2 is widely used in water and air purification. It absorbs light up to 405 nm and is a very strong oxidant (+2.25 V, pH7, SCE; +1.0 V, CH_3CN, SCE). The anatase modification of TiO_2 turned out to be essential in the photocatalytic C–H functionalization of amides.[17] The Caronna's group irradiated the semiconductor with sunlight and the electron/hole pair was able to oxidize formamide, *N*,*N*-dimethylformamide and *N*,*N*-dimethylacetamide *via* single electron transfer from the amide to the valence band of TiO_2. The one-electron oxidation is followed by deprotonation of the amides giving the corresponding radicals, which then react with heterocycles. The example with formamide and heterocycles **1** to give products **2** is shown in Scheme 1. The method was further extended to the functionalization of heterocycles using cyclic ethers (Scheme 2).[18] Both reactions are oxidative C–C bond formations utilizing only the oxidation power of the photogenerated holes. Hydrogen peroxide is added to accept the excess electron.

The oxidation of THF and 2,5-dihydrofuran (DHF) by UV light-excited ZnS (1.82 V *vs.* NHE, pH 7) was reported by the Kisch group.[19] The unsaturated cyclic ether DHF undergoes the ZnS-photocatalyzed one-electron oxidation

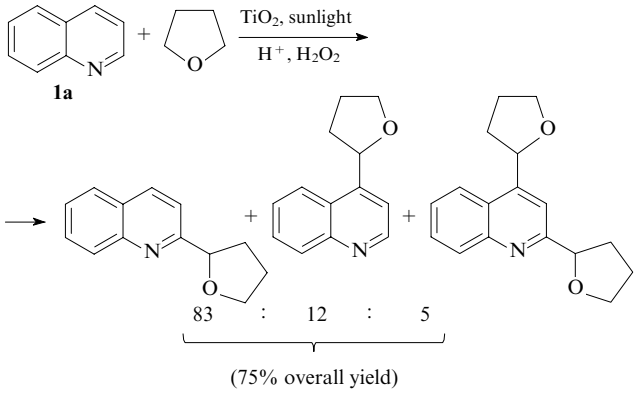
Scheme 1



1a–d **2a–d**

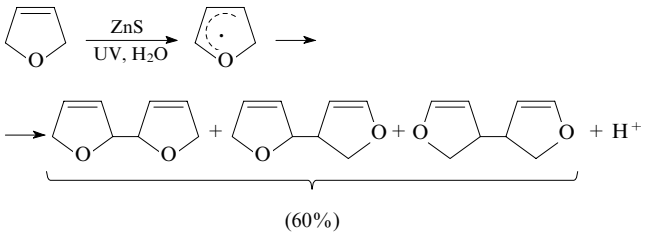
Compound **1**	X^1	R^1	Compound **2**	X^2	R^2	Yield (%) (GC data)
a	CH	H	**a**	CH	$C(O)NH_2$	90
b	CH	Me	**b**	$CC(O)NH_2$	Me	100
c	CMe	H	**c**	CMe	$C(O)NH_2$	69
d	N	H	**d**	N	$C(O)NH_2$	42

Scheme 2



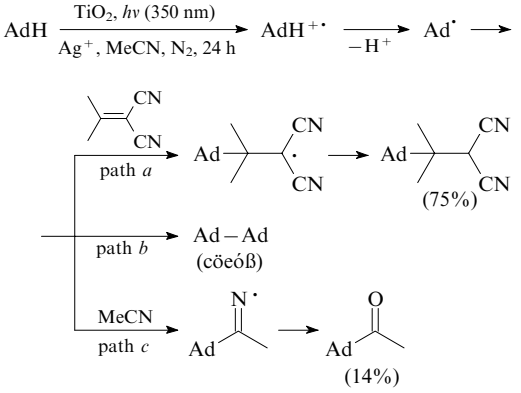
and deprotonation 10 times faster compared with the photocatalytic THF oxidation. Both substrates form dimers as shown in Scheme 3. The reductive half-reaction leads to the formation of hydrogen, which has been monitored during the reaction.

Scheme 3



Another example of TiO_2 heterogeneous photoredox catalysis is the C–C bond formation between an electrophilic alkene and adamantane (AdH).[20] After 24 h of irradiation, the target product was formed in only 35% yield (Scheme 4, path *a*). By adding silver sulfate as a sacrificial electron acceptor, the yield was increased to 75% (Scheme 4, path *a*). The reduced silver is removed during the workup by filtration and chromatography. As in the previously discussed examples, the single electron transfer oxidation of adamantane is followed by deprotonation leading to the 1-adamantyl radical, which couples with isopropylydenemalononitrile (IPMN) (see Scheme 4, path *a*). Without the coupling reagent, 1-adamantyl radicals dimerize in trace amounts (see Scheme 4, path *b*) or are coupled with CH_3CN used as a solvent leading to 1-adamantyl methyl ketone (14% yield) *via* the iminyl radical (Scheme 4, path *c*).

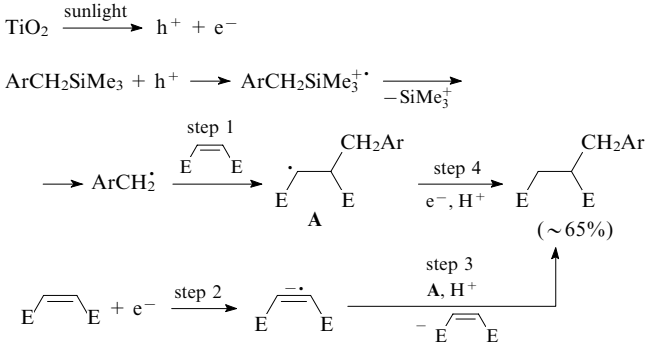
Scheme 4



Ad is 1-adamantyl

The activation of Si–C bonds, for example in benzyl(trimethyl)silanes occurs more easily than C–H activation. Being a good electrofugal group, trimethylsilyl is prone to leave the molecule after one-electron photooxidation by a suitable heterogeneous semiconductor. This principle was implemented in the radical alkylation of electrophilic olefins.[21] 4-Methoxybenzyl (trimethyl)silane (E_{ox} = 1.31 V *vs.* SCE in CH_3CN) serves as a single electron donor to the valence band of excited TiO_2. The electrophilic olefin plays the role of either a radical trap (Scheme 5, step 1) or electron acceptor from the conduction band of TiO_2 (see Scheme 5, step 2). This in turn facilitates the reaction route to the desired product (E_{red} = −0.84 V *vs.* SCE in CH_3CN for maleic acid or maleic anhydride). Radical adduct **A** is reduced by the radical anion (see Scheme 5, step 3) or by electron transfer from the conduction band of the TiO_2 semiconductor (see Scheme 5, step 4) and is protonated by water present in the solvent to give the final products.

Scheme 5



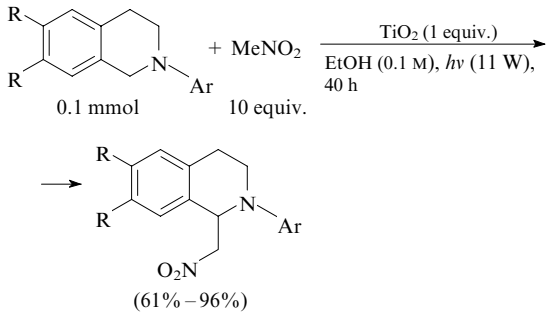
Ar = 4-$MeOC_6H_4$; E = CO_2H or E–E = $(CO)_2O$

The UV light-absorbing semiconductor TiO_2 proved to be an alternative to homogeneous photoredox-active organic dyes that were used in aza-Henry and Mannich reactions, in C–P and other C–C bond formation reactions (Scheme 6).[22] The reaction starts with the easy oxidation of the tertiary amines, here tetrahydroisoquinoline (THIQ), which forms highly reactive iminium ion intermediates after one-electron oxidation by a photoexcited semiconductor. The reductive half-reaction was not investigated in detail by the authors, but it may be expected that dihydrogen is produced or components in the reaction mixture, *e.g.*, nitromethane, are reduced. The heterogeneous photocatalysts can be reused and proved to be effective even after five consecutive photocatalytic reactions in the case of the aza-Henry reaction with TiO_2.

Chiral metal-organic frameworks (MOFs) merge the properties of photoredox catalyst and organocatalyst.[23] Two independent units of L- or D-pyrrolidin-2-ylimidazole (PYI) serve as organocatalysts and triphenylamine is incorporated as a photoredox active group into a solid framework that makes the system heterogeneous. The new porous metal-organic framework consists of a two-dimensional brick wall layered structure built of three connected binuclear zinc nodes and 4,4′,4″-nitrilotribenzoate bridges. Two investigated metal-organic frameworks Zn-PYI1 and Zn-PYI2 are mirror images that give identical products with inverse configuration. When producing these MOFs

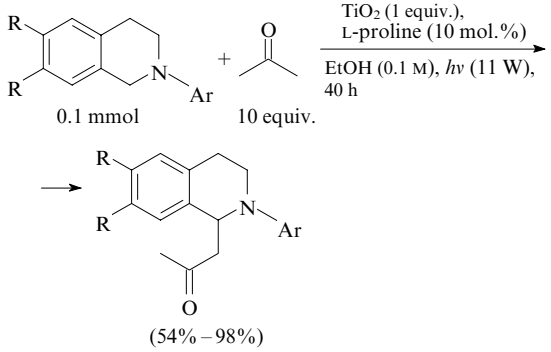
Scheme 6

Oxidative aza-Henry reaction



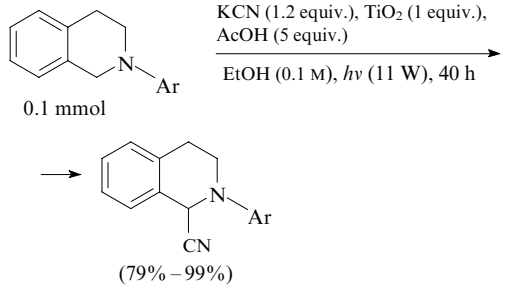
R = H, OMe; Ar = Ph, 4-MeOC$_6$H$_4$, 4-FC$_6$H$_4$, 2-MeC$_6$H$_4$, 2-naphthyl, *etc.*

Oxidative Mannich reaction



R = H, OMe; Ar = Ph, XC$_6$H$_4$ (X = 4-MeO, 4-F, 4-Me, 3-MeO, *etc.*)

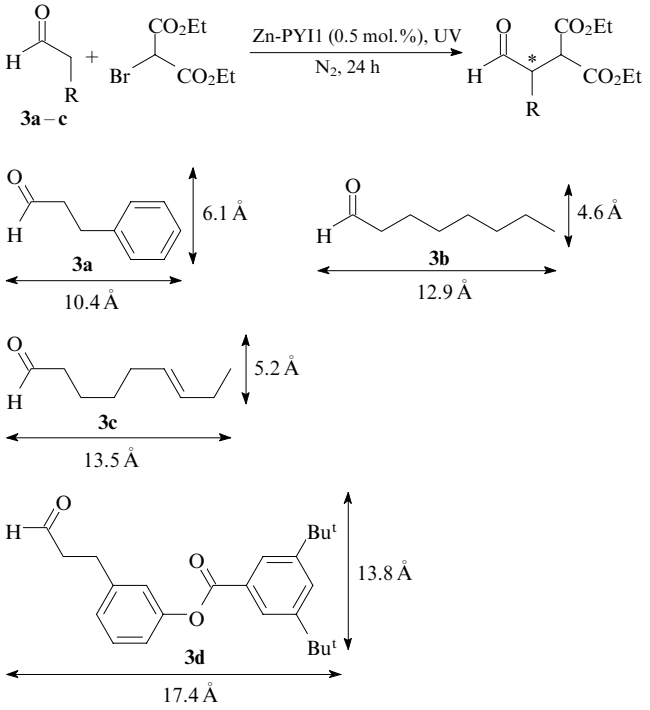
Oxidative cyanation



Ar = Ph, 4-MeOC$_6$H$_4$, 4-FC$_6$H$_4$, 3-MeOC$_6$H$_4$, *etc.*

L-*N*-*tert*-butoxycarbonyl-2-(imidazole)-1-pyrrolidine was used for Zn-PYI1 and D-*N*-*tert*-butoxycarbonyl-2-(imidazole)-1-pyrrolidine was used for Zn-PYI2. The two heterogeneous photo-organocatalysts absorb at 350 nm and the redox potential of the excited state Zn-PYI1$^+$/Zn-PYI1* (or Zn-PYI2$^+$/Zn-PYI2*) couple was estimated as -2.12 V *vs*. SCE being more negative than that of diethyl 2-bromomalonate ($E^0 = -0.49$ V), a well-known α-alkylation agent.[24] The successful reaction between diethyl 2-bromomalonate and phenylpropanal (**3a**), octanal (**3b**) or (*E*)-non-6-enal (**3c**) gave 74% (92%), 65% (86%) and 84% (92%) yield (*ee*), respectively (Scheme 7, aldehydes **3a**, **3b** and **3c**). The pore size of the Zn-PYI1 catalyst is large enough to allow all these substrates to pass through, but the more bulky aldehyde **3d** are larger than the pore size of Zn-PYI1, resulting in only 7% of α-alkylation product under the same reaction conditions. The size selectivity of the substrate indicates that the alkylation reactions occurred mostly in the channel of the catalyst, but not on the external surface.

Scheme 7

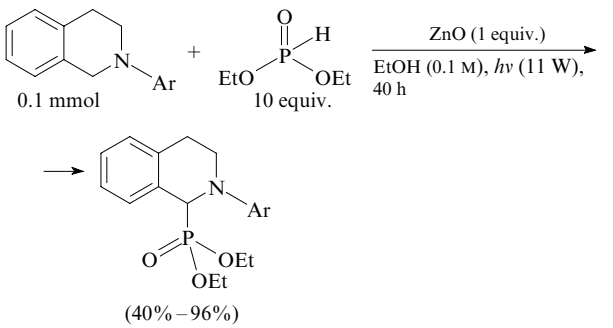


2. Carbon–heteroatom bond forming reactions

a. C–P bond forming reactions

Zinc oxide is another well-known UV light-absorbing semiconductor. The material was used to catalyze a C–P bond formation reactions described previously by König's group.[25] As discussed above, the one-electron oxidation of the tertiary amine (tetrahydroisoquinoline) by ZnO under irradiation allows coupling with diethyl phosphonate (Scheme 8).[26] Recycling experiments showed that the photocatalyst is effective for four subsequent reaction cycles.

Scheme 8



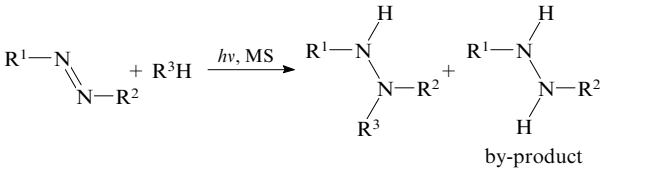
Ar = Ph, XC$_6$H$_4$ (X = 4-MeO, 4-F, 4-Me, 3-MeO), *etc.*

b. C–N bond forming reactions

In a modification of the above mentioned ZnS-photocatalyzed dimerization of 2,5-dihydrofuran (described in Section III.1), the reactive radical intermediates were trapped by azobenzene to form a C–N bond yielding an allylhydrazine.[27] This method of photocatalyzed C–N bond formation is suitable for a range of 1,2-diazenes in combi-

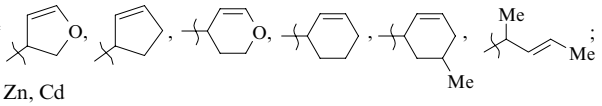
nation with cyclic allyl or enol ethers and olefins as shown in Scheme 9.

Scheme 9



$R^1 = R^2 = Ph$, 4-MeC_5H_4; $R^1 = Bu^t$, $R^2 = Ph$;

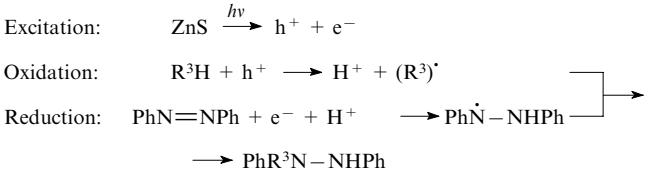
R^3 =



M = Zn, Cd

Difficulties in the purification process of the compounds led to low isolated yields (10%–40%) compared to the yields determined by HPLC. A strong solvent dependence was observed for this photocatalytic process; the reaction proceeds fast in pure methanol or mixtures of methanol or water with n-hexane or THF, while no reaction could be observed in dry solvents. The irradiation was performed with a high-pressure mercury lamp. In the case of 1-*tert*-butyl-2-phenyldiazene, only one product isomer could be observed, which can be explained by the higher stability of the phenyl-substituted hydrazyl radical compared to the *tert*-butyl-substituted one. The investigations of Kisch's group led to the mechanistic proposal given in Scheme 10.[27]

Scheme 10



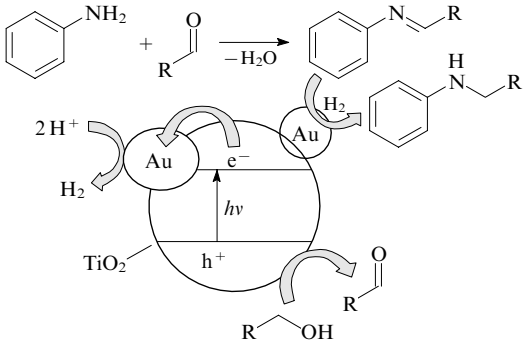
The first excitation step leads to an electron/hole pair formation in the semiconductor. The ether or olefin radical in the oxidative half-reaction can be formed stepwise from the initial radical cation by deprotonation or *via* a simultaneous process where electron transfer is coupled with deprotonation. The hydrazyl radical in the reductive part forms *via* electron transfer to 1,2-diazene coupled with protonation. The reaction is a typical example of a type B heterogeneous photocatalysis.

Another principle of C–N bond construction was implemented when mixtures of primary alcohols and primary amines were irradiated with UV light in the presence of TiO_2 loaded with Pd (Ref. 28) or Au (Ref. 29) nanoparticles.

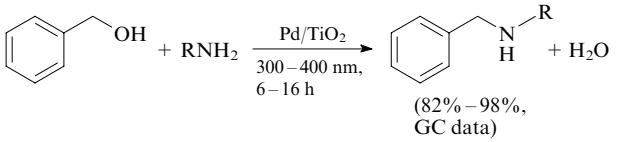
The mechanism proposed by Stibal *et. al.*[29] for the formation of secondary amines using Au/TiO_2 and Pd/TiO_2 includes one-electron oxidation of the primary alcohol and subsequent condensation of the resulting aldehyde and amine, which is not photocatalytic (Scheme 11).

The alcohol oxidation can proceed *via* direct oxidation by holes from the valence band of the photocatalyst or indirectly *via* $OH^•$ radicals formed in the reaction of OH^- ions with surface holes. Further hydrogenation of the imine double bond involves molecular hydrogen that is formed from protons on Au or Pd nanoparticles and electrons from the conduction band of the excited TiO_2. Particle size is

Scheme 11

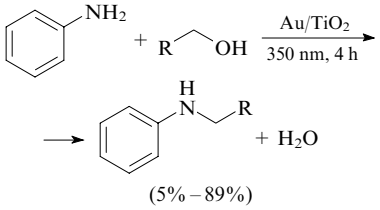


Scheme 12



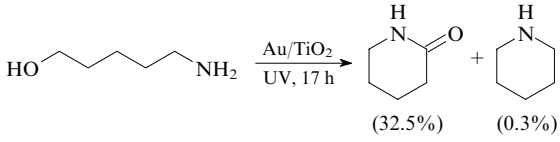
R = Bu^n, 3-MeC_6H_4, 3-$MeOC_6H_4$, 3-ClC_6H_4, *etc.*

Scheme 13



R = H, Me, Et, Pr^n, n-C_5H_{11}

Scheme 14



crucial for the successful process with the optimum being around 5 nm for Au nanoparticles and around 2.5 nm for Pd nanoparticles. Schemes 12 and 13 represent the scope of the substrates when palladium and gold nanoparticles, respectively, are used. Moreover, the Au/TiO_2 photocatalyzed cyclization of 5-aminopentanol resulted in an acceptable yield of δ-valerolactam (Scheme 14), which shows that the method can in principle be applied to the synthesis of commercially valuable lactams and heterocyclic amines.

c. C–O bond forming reactions

To pursuit the synthesis of fine chemicals, the group of Matsumuro investigated photocatalytic epoxidation of olefins over TiO_2 under UV light irradiation, as epoxides are valuable intermediates for polymer synthesis.[30] The construction of C–O bonds requires the presence of O_2 in the reaction mixture. The epoxidation of hex-1-ene, dec-1-ene and hexadec-1-ene proved to be selective giving the corresponding epoxides as almost single products when TiO_2 in the anatase modification was used as the photocatalyst. This could be explained by the high capability of anatase

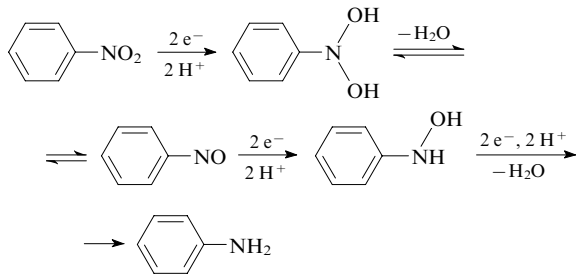
TiO_2 to adsorb oxygen as a component for a successful photocatalytic process. The chemical yield of the epoxide products increases with shorter olefin chains to reach 79% in the case of hex-1-ene, while dec-1-ene gave 68% and hexadec-1-ene gave 42% of the corresponding 1,2-epoxides. According to the oxidation potentials of starting olefins, which are in the range of 0.98–1.0 V *vs.* Ag/AgCl (CH_3CN) the photogenerated holes in the valence band of TiO_2 are able to oxidize them to the corresponding radical cations with subsequent oxidation by oxygen yielding the desired epoxides.

IV. Visible light-mediated heterogeneous photocatalysis

1. Photoreduction of nitro groups

The photocatalytic reduction of nitrobenzene derivatives has been investigated in detail including visible light-mediated heterogeneous photocatalysis. This N–H bond formation from N–O bonds is a 6-electron plus 6-proton reaction process (Scheme 15). Different heterogeneous photocatalysts such as Ru(II) dye-sensitized TiO_2,[31] Ru(II) dye-sensitized urea-modified TiO_2 [32] and $PbBiO_2X$ (X = Br, Cl, I) [33] were applied for the photocatalytic reductions of nitrobenzene derivatives to the corresponding anilines.

Scheme 15

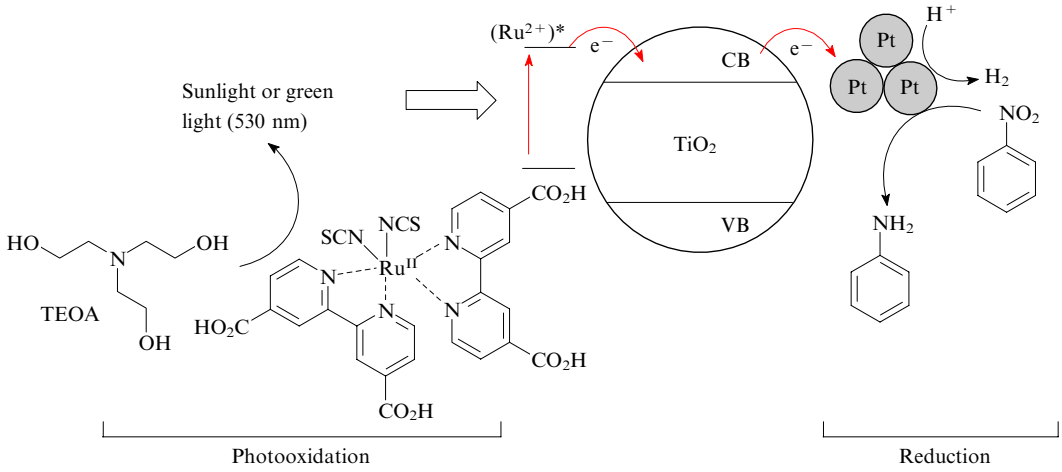


Ru(II) dye-sensitized TiO_2 is the active part of the Grätzel solar cell [34] possessing an absorption maximum in the green region of the solar spectrum that has the highest intensity. This heterogeneous semiconductor mediates the reduction reaction well if an appropriate amount of transition metal nanoparticles with appropriate particle size is present. The metal nanoparticles are obtained by photocatalytic reduction of Pt(II), Pt(IV), Pd(II), Ag(I) or Au(III) salts.[31] The formed clusters serve (i) as electron acceptors for the conduction band of the excited dye-sensitized TiO_2 (Scheme 16), which further generate dihydrogen by reduction of protons provided from the photocatalytically oxidized triethanolamine (TEOA) and (ii) as hydrogenation catalysts for the organic substrates. Systematic variation of the transition metals, their amounts and the method of their reduction revealed a relationship between the nature of the metal and the optimal catalytic amount. The most promising results with almost quantitative nitrobenzene conversion were obtained by using Pt colloids (10^{-1}–10^{-6} mol.%), Au(III) salts (10^{-1}–10^{-4} mol.%) and Pt(II) and Pd(II) salt (and 0.05–0.01 mol.%) (Scheme 16). The amount of the metal nanoparticle catalyst with a concentration of more than 1 mol.% led to low degrees of conversion in all metal salt cases. An investigation of the morphology of the formed transition metal particles by transmission electron microscopy revealed that the catalytically active particles have a typical size below 20 nm.

Using one of the best working catalyst precursors, K_2PtCl_6, the range of substrates was extended to perform the photocatalytic reduction of aldehydes. The experiments indicated that it is necessary to optimize the salt concentration according to every substrate: ethyl 4-nitrobenzoate, 4-nitrobenzonitrile, 4-nitrobenzaldehyde, 4-bromonitrobenzene, 1,4-dinitrobenzene, 1,2-dinitrobenzene, 2-nitroacetophenone and so on.

Later, an enhanced photocatalytic activity of Ru(II)/TiO_2 heterogeneous photocatalyst in nitroarene reductions in the presence of urea derivatives was found.[32] Urea itself serves as a proton transfer mediator. The oxidation of TEOA by the photocatalyst provides the electrons and protons necessary for the nitrobenzene reduction. Their transfer to the nitroarene substrate may be the rate-determining step. The investigation showed that the addition of urea derivatives accelerates the proton transfer thus facilitating the use of TiO_2-based photocatalysts in nitroarene reduction. It was found that urea, thiourea, *N*,*N*-dimethylurea and tetramethylurea in an amount of 10^{-4} mol.% (with respect to nitrobenzene) lead to almost quantitative conversion of nitrobenzene in the photocatalytic system (see Scheme 16, an urea derivative is present instead of Pt nanoparticles). The method also enhances the conversion of 4-cyano, 4-bromo- and 4-ethoxycarbonyl-nitrobenzenes to

Scheme 16



the corresponding anilines when using 10^{-4} mol.% of thiourea in the reaction mixture.

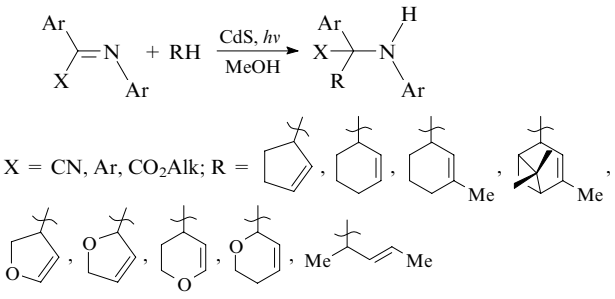
Semiconductors of the composition $PbBiO_2X$ (X = Br, Cl) were also used for the photocatalytic reduction of nitrobenzene derivatives under visible-light irradiation. The heterogeneous semiconductor is coloured and absorbs visible light without any additional sensitization.[33] The visible-light absorption is caused by the narrow band gap of the materials that is in range of 2.47–2.55 eV (see Fig. 2). These solid materials have a layered structure consisting of $[PbBiO_2^+]$ layers formed by metal–oxygen covalent bonds, which are separated by halide layers. The metal atoms reach the outer crystal surface and become, therefore, accessible for the catalytic process. When used for the same photocatalytic nitrobenzene reduction with blue light irradiation, $PbBiO_2Br$ and $PbBiO_2Cl$ promoted almost full conversion of nitrobenzene to aniline as the single major product (monitored by gas chromatography); no urea derivatives or metal nanoparticles are required in the process. Moreover, the recycled $PbBiO_2Br$ semiconductor promoted the nitrobenzene photocatalytic reduction for up to 5 cycles without any loss in efficacy and is applicable for photocatalytic reduction of a wide range of nitrobenzene derivatives *e.g.*, 4-hydroxy, 4-ethoxycarbonyl, 4-cyano, 4-nitro- and 4-formylnitrobenzenes, 1,4-dinitrobenzene and so on (a total of twelve examples reported) with moderate to excellent yields.

2. Carbon–carbon bond forming reactions

The material most used in reactions of this type is the semiconductor CdS. With an appropriate band gap (2.4 eV) and oxidation potential (+1.5 V *vs.* SCE, CH_3CN), this semiconductor was thoroughly investigated by Kisch *et al.*[2,5] A limitation of the semiconductor is its easy photocorrosion. The dimerization of 2,5-dihydrofuran by one-electron oxidation *via* excited ZnS was already mentioned in section III.1 (see Scheme 3). Replacing ZnS by CdS allows for the excitation by visible light. The product distribution is unchanged.

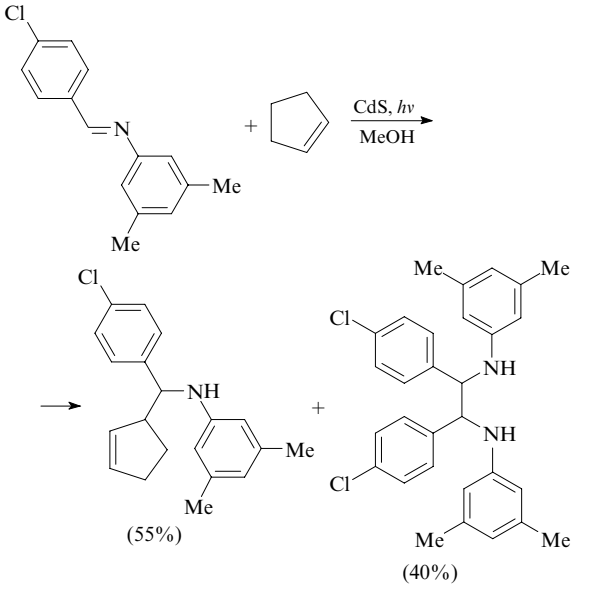
The 2,5-dihydrofuryl radical can be further employed in C–C heterocoupling reactions with imines. Moreover, the substrates that undergo one-electron oxidation include different allyl/enol ethers and olefins. The resulting homoallylimines can be obtained in 30%–75% yields when trisubstituted imines are used in the photocatalytic cycle (Scheme 17).[35–37]

Scheme 17



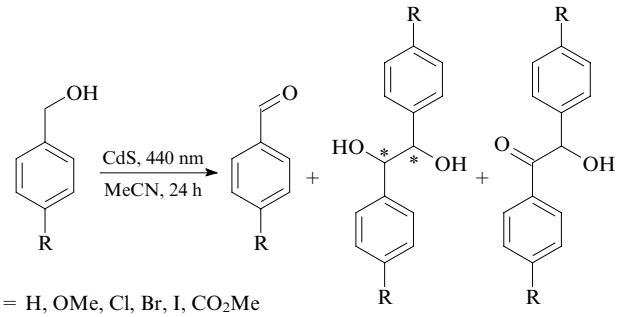
A disubstituted imine in the same photocatalytic reaction with cyclopentene gives the hydrodimer along with the desired homoallylamine (Scheme 18).[38] Its formation suggests a parallel one-electron reduction process from the conduction band of the excited photocatalyst to the imine affording the α-aminobenzyl radical, which couples with an allylic radical formed from the olefin *via* oxidative electron transfer and deprotonation.

Scheme 18



Polycrystalline CdS was found to be effective in the oxidative coupling of a series of benzyl alcohols with benzyl amines.[39] Irradiation of an oxygen-free suspension of CdS and primary benzyl alcohol derivatives dissolved in acetonitrile with blue light for 24 h gave substituted benzaldehyde, hydrobenzoin (as a mixture of diastereomers) and benzoin as products (Scheme 19). As a by-product, hydrogen is produced in the conduction band of the excited CdS using the remaining electrons of the photocatalytic cycle. Previous studies reported hydrogen gas formation at Pt nanoparticles on platinized CdS converting protons with the help of accumulated electrons from the conduction band.[40] The photocatalytic reaction is strongly dependent on temperature and initial primary benzyl alcohol concentration. Scheme 20 shows the mechanism proposed for this process.

Scheme 19



Scheme 20

$$ArCH_2OH + h^+ \longrightarrow ArC^{\bullet}H(OH) + H^+$$

$$2\,ArC^{\bullet}H(OH) \longrightarrow ArCH(OH)CH(OH)Ar$$

$$2\,ArC^{\bullet}H(OH) \longrightarrow ArCHO + ArCH_2OH$$

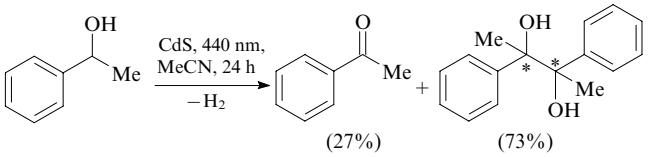
$$ArC^{\bullet}H(OH) \longrightarrow ArCHO + e^- + H^+$$

$$ArC^{\bullet}H(OH) + h^+ \longrightarrow ArCHO + H^+$$

$$2\,H^+ + 2\,e^- \longrightarrow H_2$$

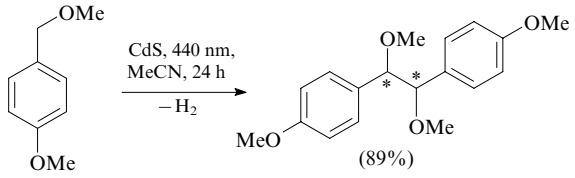
When secondary alcohols were employed under the same photocatalytic conditions, there was no formation of such product as benzoin, *e.g.*, 1-phenylethanol gave a diastereomeric mixture of 1,2-diols in 73% yield and acetophenone (27%) as a by-product (Scheme 21).

Scheme 21



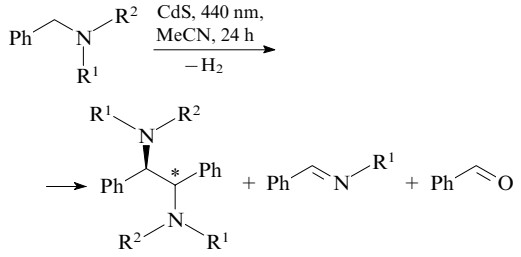
In the photocatalytic conversion of methyl *p*-methoxybenzyl ether with CdS, the homocoupling product forms almost exclusively in 89% yield (Scheme 22).

Scheme 22



When the same reaction conditions were applied to *N*,*N*-dimethylbenzylamine, it was converted to *N*,*N*,*N*′,*N*′-tetramethyl-1,2-diphenylethylenediamine and benzaldehyde. Other benzylamine derivatives gave the desired C–C homocoupling products with benzaldehyde or imine as by-products (Scheme 23).

Scheme 23

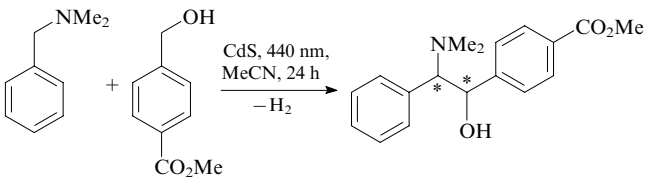


meso + *rac*
(16%–96%, according to NMR and GC data)

R^1 = H, Me, Bn; R^2 = H, Me, Pr^n

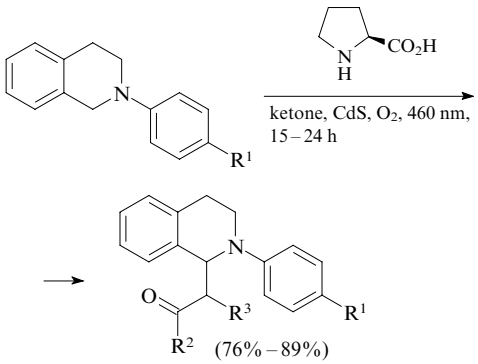
Since the photocatalytic homocoupling of benzylamines and benzyl alcohols gave promising results, it was interesting to combine them with the aim of obtaining cross-coupling 1,2-aminoalcohol products (Scheme 24). Along with the desired cross-coupling product, homocoupling products from benzylamine and benzyl alcohol were found. The reaction requires further optimization to become applicable to a wider range of starting materials.

Scheme 24



As mentioned in Section III.1, tertiary amines are good substrates for one-electron oxidation processes and, particularly, for transformation of tetrahydroisoquinolines efficiently induced by TiO_2 photocatalysts (see Scheme 6).[22] Almost at the same time, a Mannich type reaction of *N*-aryltetrahydroisoquinolines with ketones employing L-proline as the organocatalyst and CdS as a photoredox catalyst upon irradiation with blue light LED (460 nm) was investigated [6] (Scheme 25).

Scheme 25

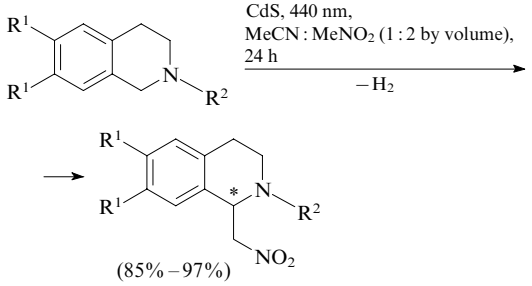


R^1 = H, OMe; R^3 = H: R^2 = Me, Et; $R^2–R^3$ = $(CH_2)_4$;
ketone is acetone, butan-2-one or cyclohexanone

The product yields range from 76% to 89% with the neat ketone being used as a solvent. The amount of ketone could be reduced to a 2- to 10-fold excess by using acetonitrile as a solvent.

Switching from TiO_2 to CdS (see Section III.1) allowed sensitization of the catalyst by a visible light source (440 nm LEDs), the desired products being formed in 85%–97% yields (Scheme 26).[39]

Scheme 26

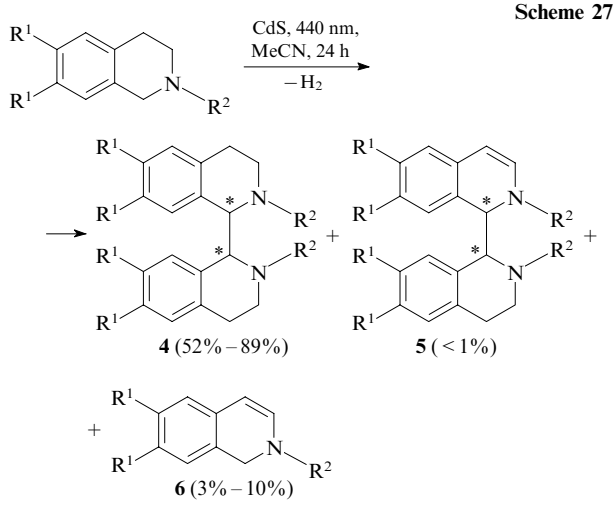


R^1 = H, OMe; R^2 = Ph, 4-BrC_6H_4

When no nucleophile is present in the reaction mixture, the radicals are homocoupled to form dimers **4** in 52%–89% yields along with trace amounts of dehydrodimers **5** and dihydroisoquinoline **6** (Scheme 27).[39]

The preparation of enantiomerically enriched molecules is always an important goal in organic synthesis. Combining photoredox catalysts with organocatalysis provides an elegant way to achieve this goal and the method can be employed for homogeneous as well as heterogeneous systems. An interesting way of merging the favourable properties of homogeneous dyes with the advantages of heterogeneous systems (easy recovery, *etc.*) is the immobilization of photoredox active dyes on solid supports (*e.g.*, TiO_2, SiO_2). This method makes use of the redox power of soluble organic dyes known to be effective in photocatalysis

Scheme 27



R^1 = H, OMe; R^2 = Ph, 4-BrC_6H_4

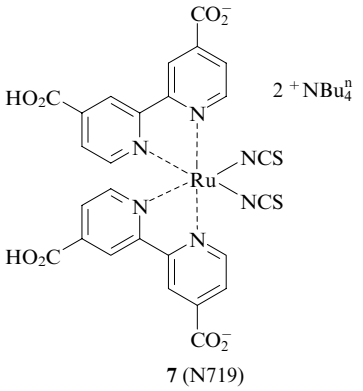
[*e.g.*, Eosin Y, Ru(II) and Ir(III) dyes or Cu(I) complexes, *etc.*] in a heterogeneous manner.

Recently [41] this approach was used for a photooxidative Michael addition/oxyamination under visible light irradiation. The photosensitizer N719 (structure **7**) immobilized on TiO_2 surface together with (*S*)-2-[diphenyl(trimethylsilyloxy)methyl]pyrrolidine as an organocatalyst afforded the α,β-substituted aldehydes in good to excellent yields (30%–80%) with high diastereo- and enantioselectivities (90%–99%).

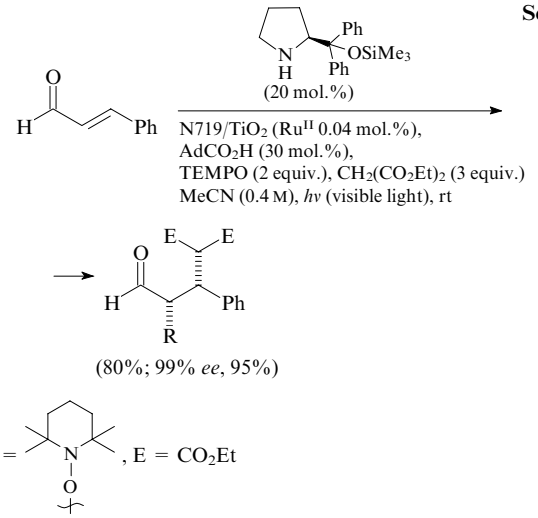
It was found that 0.04 mol.% of the immobilized dye with respect to the starting α,β-unsaturated aldehyde is sufficient to provide an excellent (80%) yield under optimized conditions (Scheme 28).

The optimized conditions comprise the addition of adamantanecarboxylic acid, which promotes the formation

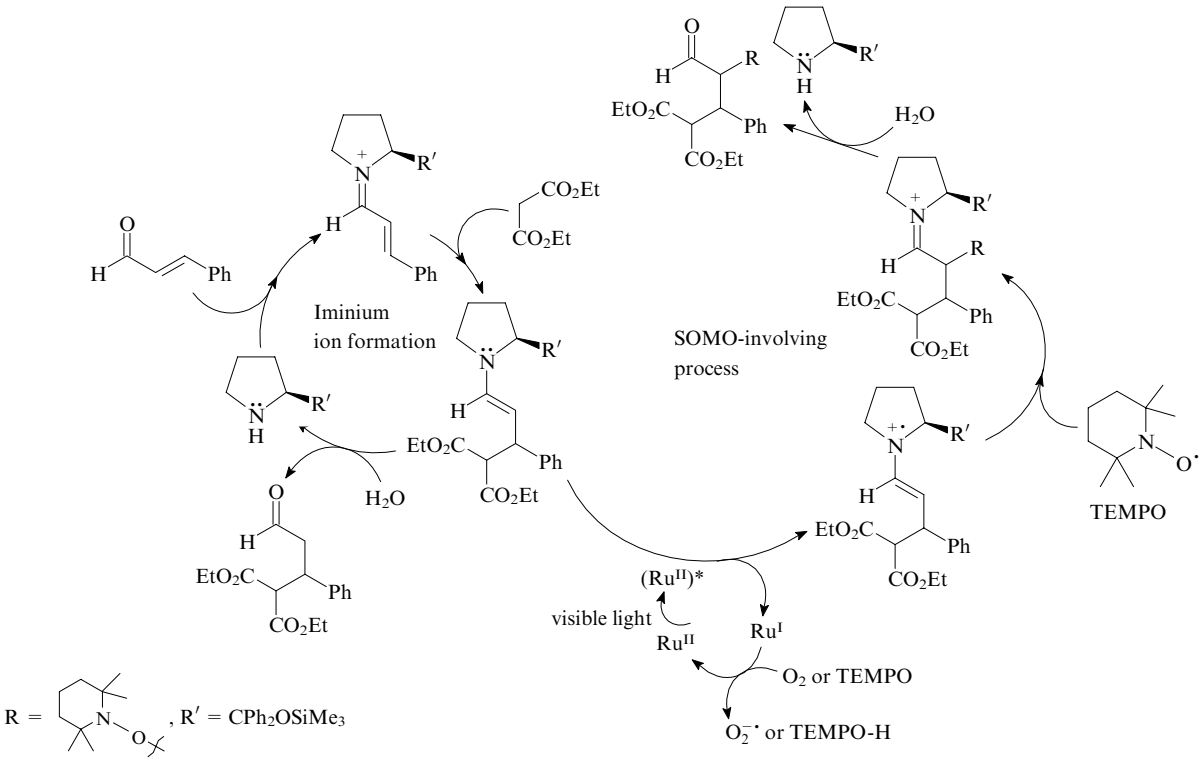
Structure 7



Scheme 28



Scheme 29

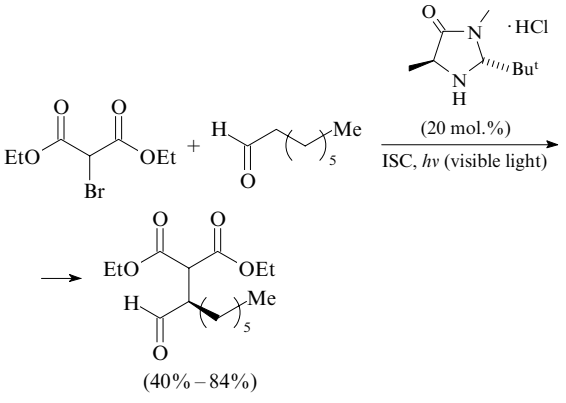


of the iminium ion from the starting aldehyde, and the chiral organocatalyst according to the mechanism given in Scheme 29 where the enantioselectivity of β-position is determined by the iminium ion formation step and the enantioselectivity of the α-position is directed by the chiral intermediate in the photocatalytic process involving the SOMO (single occupied molecular orbital) of the radical cation in the second step. Moreover, even if heterogeneous TiO_2 serves only as the solid support to the visible light-absorbing N719 dye, the reaction is less efficient when the two separate catalysts are used.

In order to develop photocatalytically more active semiconductors that absorb visible light, Huang's group designed a new layer-structured $PbBiO_2Br$ compound with 2.3 eV band gap energy.[42] The material turned out to be much more active in methyl orange and methylene blue degradation experiments in comparison to already known visible-light absorbing $PbBi_2Nb_2O_9$, $TiO_{2-x}N_x$ and BiOBr semiconductors. These semiconductors are characterized by 2.6, 2.88 and 2.9 eV band gaps, respectively.[42] Cherevatskaya *et al.*[6] obtained $PbBiO_2Br$ in two crystal modifications as bulk crytals and as nanocrystals with 0.17 $m^2\ g^{-1}$ and 10.8 $m^2\ g^{-1}$ specific surface areas, respectively, and employed in visible-light-promoted stereoselective alkylation of aldehydes. The enantioselective C–C bond construction by the reduction of halogen precursors explored earlier in the MacMillan's group[24] was investigated using visible light-excited semiconductor photocatalysts. Several semiconductors were compared in a model α-alkylation of octanal (Scheme 30) where the enantioselectivity was induced by a chiral secondary amine. Apart from the promising $PbBiO_2Br$ material in nanocrystal and bulk crystal modifications, the well-known TiO_2 as unmodified P25 Degussa and surface-modified catalysts were involved in the photocatalysis. The surface-modified TiO_2 was prepared *via* immobilization of the visible light-responsive redox active Phos-Texas-Red dye (λ_{max} = 578 nm) on the semiconductor surface (structure **8**). The UV measurements indicate that the amount of surface-immobilized dye was 1.2 mol.% with respect to the halogen precursor.

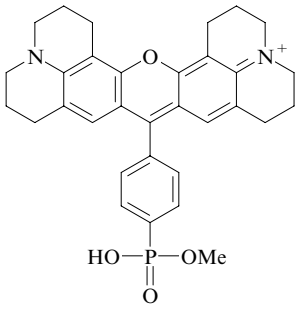
All used semiconductors have more negative reduction potential than the halogen precursors, thus enabling the single electron transfer from the conduction band of the excited photocatalyst to cleave the C–Br bond. The product yield depends on several parameters, *e.g.*, the specific surface area, the reaction temperature and the visible-light

Scheme 30



ISC is inorganic semicondor

Structure 8



8 (Phos-Texas-Red)

absorption. $PbBiO_2Br$ semiconductors were used in two particle sizes, and the smaller nanometre-sized particles with larger specific surface area gave a better product yield. Unmodified Degussa P25 TiO_2 with an even larger surface area of 50 $m^2\ g^{-1}$ gave low yields, due to its weak absorption in the visible-light region. TiO_2 surface modification with a green-light absorbing dye extends the absorption into the visible wavelength range of 530 nm (high-power LED radiation) but the yield remains largely unchanged. By lowering the reaction temperature from room temperature to −10 °C, the yield for the same reaction time is decreased by 15%–30% in almost all cases but the enantioselectivity is slightly increased. The light penetration path length is crucial. Transferring the heterogeneous reaction mixture from a batch reactor into 1 mm diameter tubes increases the yields dramatically within even shorter irradiation time. Recycling experiments showed the possibility to use the recovered TiO_2 semiconductor in additional photocatalytical reactions with no loss in product yield. The established method is useful for other halogen precursors such as 2,4-dinitrobenzyl bromide and bromoacetophenone giving somewhat lower product yields (72% and 65%, respectively).

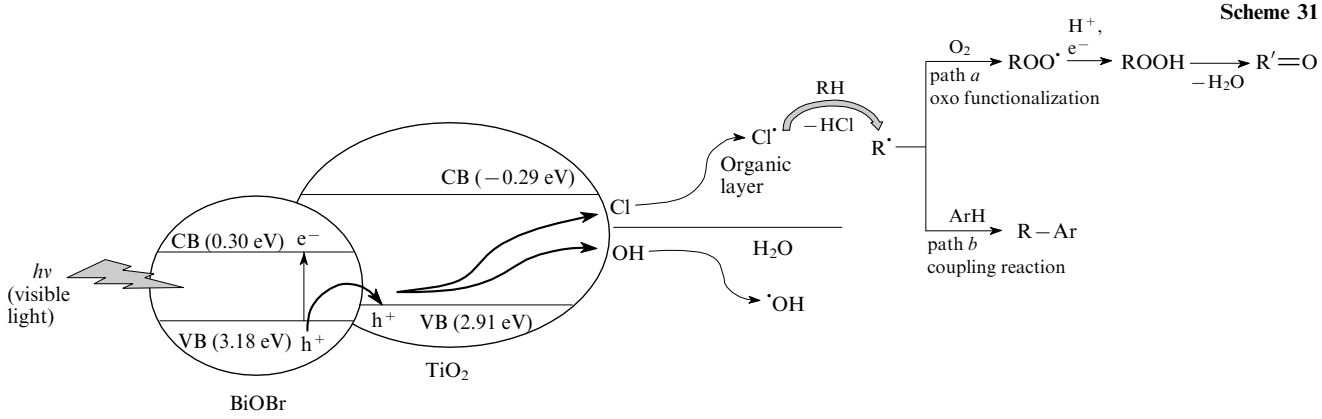
3. Carbon–heteroatom bond forming reactions

a. C–O bond forming reactions

An interesting approach to C–H bond transformation, which is a rather diffucult task, was used by Fu *et al.*,[43] who combined several semiconductors with the aim to enhance their photocatalytic properties. Visible light-sensitive BiOBr has a narrower band gap of 2.88 eV (TiO_2 has 3.2 eV) and a lower valence band upper edge energy (3.18 eV *vs.* NHE, pH 7) than TiO_2 (2.91 eV *vs.* NHE, pH 7). As depicted in Scheme 31, the holes from the VB of visible light-excited BiOBr can thus migrate to the VB of TiO_2 due to the 0.27 eV difference between the oxidation potentials of these two semiconductors. The TiO_2 then acts as the active one-electron oxidizing agent to produce chlorine radicals or hydroxyl radicals from the chlorine or hydroxyl groups that are chemisorbed on the surface. Free chlorine radicals as major participants in the organic layer eliminate hydrogen atoms from alkanes to afford alkyl radicals, which react with O_2 under aerobic conditions to form almost exclusively ROO$^{\bullet}$ radicals (see Scheme 31, path *a*). The peroxy radicals are then reduced with electrons from the conduction band (CB), and protonation leads to the formation of the peroxy acid, which in turn forms aldehydes and ketones after dehydration as the major products of this reaction.

The method was applied to aromatic and cyclic aliphatic hydrocarbons including cyclohexane, toluene, ethylbenzene

Scheme 31

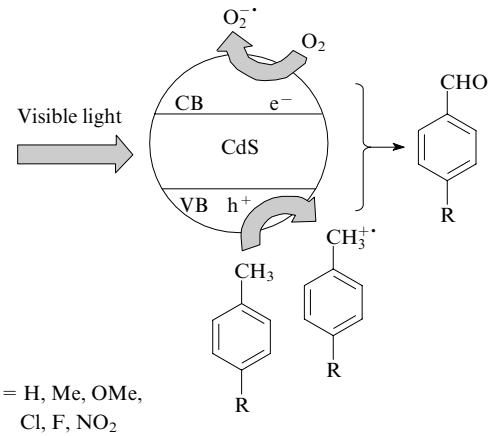


RH = cyclo-C_6H_{12}, PhMe, PhEt, *p*-$Me_2C_6H_4$; R′ = R − H

and *p*-xylene yielding cyclohexanone, benzaldehyde, acetophenone or *p*-methylbenzaldehyde, respectively. The generated alkyl radicals could be further applied in C−C bond construction reactions, which would allow the direct functionalization of hydrocarbons without preliminary activation *via* functional groups (see Scheme 31, path *b*).[43]

Another case of challenging C−H transformation into C−O bond was investigated by Xu's group.[44] The activation of inert C−H bonds can result in poor degree of conversion, selectivity and overoxidation as observed in toluene and saturated hydrocarbon photooxidation experiments using TiO_2 with UV light irradiation.[45–47] In order to prevent the formation of undesired products and use mild photocatalytic conditions for C−O bond construction, the researchers[44] synthesized photoeffective CdS semiconductors with (i) a specific sheet structure morphology with cubic phase crystallinity (1.9 nm crystals), (ii) high surface area (132 $m^2\ g^{-1}$) and (iii) efficient separation of photogenerated charges upon visible light irradiation. This newly prepared CdS semiconductor has a narrower band gap of ~2.2 eV and showed 100% selectivity in the catalytic photooxidation of toluene and toluene derivatives to the corresponding aldehydes under visible light irradiation (Scheme 32). The yields of the target products after 10 h of irradiation remain moderate (27%–39%) but could be increased by using longer irradiation time. Also the photocatalyst is stable and reusable at least for four photocatalytic cycles in the selective oxidation of toluene with the same 33% yield of benzaldehyde. The proposed mechanism suggests that the photocatalytic oxidation of toluene and its derivatives over CdS is driven by photogenerated positive holes together with O_2 and $O_2^{-\bullet}$ as shown in Scheme 32.

Scheme 32



R = H, Me, OMe, Cl, F, NO_2

V. Conclusion

Heterogeneous photocatalysts can be effectively applied for organic synthesis. The reported scope of application extends from simple oxidation and reduction to enantioselective carbon–carbon bond forming reactions. Combining homogeneous organo- or metal catalysis with heterogeneous semiconductor photocatalysis has proven to be particular useful. Advantages of heterogeneous photocatalysts are the wide variety of accessible redox potentials, they are easy to reuse and often very photostable and readily available. However, several aspects in the application of heterogeneous photocatalysts are still challenging and need future improvement to broaden their application in organic synthesis. The number of suitable inorganic semiconductors with well characterized physical properties, including the valence and conducting band energies in different solvents, is still limited. Our understanding of the detailed photocatalytic mechanisms is for many reactions limited, as investigations at the interface between the catalyst surface and the homogeneous reaction medium are difficult. This lack of knowledge hampers a rational design and improvement of heterogeneous photocatalytic processes. Another limitation is the available redox energy of a semiconductor, which is defined by its band gap and is, therefore, correlated to the absorption wavelength. In order to use visible light, particularly sunlight with highest intensities in the blue and green region of the spectrum, but still to gain strongly oxidizing or reducing potentials, it is necessary to combine two or more semiconductors as photocatalysts.

With continuing progress in these different aspects of heterogeneous photo-redox catalysis more applications may certainly develop — from laboratory-scale synthetic steps to light-mediated medium or larger-scale solar production of chemicals.

References

1. G Ciamician *Science* **36** 385 (1912)
2. H Kisch *Angew. Chem., Int. Ed.* **52** 812 (2013)
3. A O Ibhadon, P Fitzpatrick *Catalysts* **3** 189 (2013)
4. A M Roy, G De, N Sasmal, S S Bhattacharyya *Int. J. Hydrogen Energy* **20** 627 (1995)
5. W Schindler, H Kisch *J. Photochem. Photobiol., A* **103** 257 (2007)
6. M Cherevatskaya, M Neumann, S Fmldner, C Harlander, S Kümmel, S Dankesreiter, A Pfitzner, K Zeitler, B König *Angew. Chem., Int. Ed.* **51** 4062 (2012)
7. S Suga, S Suzuki, J-i Yoshida *J. Am. Chem. Soc.* **124** 30 (2002)
8. T Shono *Electroorganic Synthesis* (New York: Academic Press, 1991)
9. L Friedman, H Shechter *Tetrahedron Lett.* **2** 238 (1961)
10. T Yoshimitsu, Y Arano, H Nagaoka *J. Am. Chem. Soc.* **127** 11610 (2005)
11. A Citterio, A Gentile, F Minisci, M Serravalle, S Ventura *J. Org. Chem.* **49** 3364 (1984)
12. D Dondi, M Fagnoni, A Molinari, A Maldotti, A Albini *Chem. – Eur. J.* **10** 142 (2004)
13. D Dondi, M Fagnoni, A Albini *Chem. – Eur. J.* **12** 4153 (2006)
14. S Angioni, D Ravelli, D Emma, D Dondi, M Fagnoni, A Albini *Adv. Synth. Catal.* **350** 2209 (2008)
15. I Ryu, A Tani, T Fukuyama, D Ravelli, M Fagnoni, A Albini *Angew. Chem., Int. Ed.* **50** 1869 (2011)
16. S Montanaro, D Ravelli, D Merli, M Fagnoni, A Albini *Org. Lett.* **14** 4218 (2012)
17. T Caronna, C Gambarotti, L Palmisano, C Punta, F Recupero *Chem. Commun.* 2350 (2003)
18. T Caronna, C Gambarotti, L Palmisano, C Punta, F Recupero *J. Photochem. Photobiol., A* **171** 237 (2005)
19. N Zeug, J Bücheler, H Kisch *J. Am. Chem. Soc.* **107** 1459 (1985)
20. L Cermenati, D Dondi, M Fagnoni, A Albini *Tetrahedron* **59** 6409 (2003)
21. L Cermenati, C Richter, A Albini *Chem. Commun.* 805 (1998)
22. M Rueping, J Zoller, D C Fabry, K Poscharny, R M Koenigs, T E Weirich, J Mayer *Chem. – Eur. J.* **18** 3478 (2012)
23. P Wu, C Cheng, J Wang, X Peng, X Li, Y An, C Duan *J. Am. Chem. Soc.* **134** 14991 (2012)
24. D A Nicewicz, D W C MacMillan *Science* **322** 77 (2008)
25. D P Hari, B König *Org. Let.* **13** 3852 (2011)
26. M Rueping, C Vila, R M Koenigs, K Poscharny, D C Fabry *Chem. Commun.* **47** 2360 (2011)
27. H Kisch *Adv. Photochem.* **26** 93 (2001)
28. Y Shiraishi, K Fujiwara, Y Sugano, S Ichikawa, T Hirai *ACS Catal.* **3** 312 (2013)
29. D Stíbal, J Sv, J A van Bokhoven *Catal. Sci. Technol.* **3** 94 (2013)
30. O T Ohno, K Nakabeya, M Matsumura *J. Catal.* **176** 76 (1998)
31. S Füldner, R Mild, H I Siegmund, J A Schroeder, M Gruber, B König *Green Chem.* **12** 400 (2010)
32. S Füldner, T Mitkina, T Trottmann, A Frimberger, M Gruber, B König *Photochem. Photobiol. Sci.* **10** 623 (2011)
33. S Füldner, P Pohla, H Bartling, S Dankesreiter, R Stadler, M Gruber, A Pfitzner, B König *Green Chem.* **13** 640 (2011)
34. J-H Yum, P Chen, M Grätzel, M K Nazeeruddin *ChemSusChem* **1** 699 (2008)
35. H Keck, W Schindler, F Knoch, H Kisch *Chem. – Eur. J.* **3** 1638 (1997)
36. M Hopfner, H Weiβ, D Meissner, F W Heinemann, H Kisch *Photochem. Photobiol. Sci.* **1** 696 (2002)
37. M Gärtner, J Ballmann, C Damm, F W Heinemann, H Kisch *Photochem. Photobiol. Sci.* **6** 159 (2007)
38. W Schindler, F Knoch, H Kisch *Chem. Ber.* **129** 925 (1996)
39. T Mitkina, C Stanglmair, W Setzer, M Gruber, H Kisch, B König *Org. Biomol. Chem.* **10** 3556 (2012)
40. Z Jin, Q Li, X Zheng, C Xi, C Wang, H Zhang, L Feng, H Wang, Z Chen, Z Jiang *J. Photochem. Photobiol., A* **71** 85 (1993)
41. H Yoon, X Ho, J Jang, H Lee, S Kim *Org. Lett.* **14** 3272 (2012)
42. Z Shan, W Wang, X Lin, H Ding, F Huang *J. Solid State Chem.* **181** 1361 (2008)
43. R Yuan, S Fan, H Zhou, Z Ding, S Lin, Z Li, Z Zhang, C Xu, L Wu, X Wang, X Fu *Angew. Chem., Int. Ed.* **52** 1035 (2013)
44. Y Zhang, N Zhang, Z-R Tang, Y-J Xu *Chem. Sci.* **3** 2812 (2012)
45. A J Maira, K L Yeung, J Soria, J M Coronado, C Belver, C Y Lee, V Augugliaro *Appl. Catal., B* **29** 327 (2001)
46. V Augugliaro, S Coluccia, V Loddo, L Marchese, G Martra, L Palmisano *Appl. Catal., B* **20** 15 (1999)
47. M Gonzalez, S Howell, S Sikdar *J. Catal.* **183** 159 (1999)